# Stability Analysis via Poincaré Map for Binary Cyclic Distillation

**Chengtian Cui** ccui@abo.fi

**Process and Systems Engineering Laboratory, Faculty of Science and Engineering,**
**Åbo Akademi University, Henrikinkatu 2, 20500, Turku, Finland**

CONTACT

LinkedIn

## INTRODUCTION

**Context.** Cyclic distillation separates vapor contacting from liquid transport. Vapor flows while liquid is retained during the VFP; liquid is displaced downward during the LFP. Under the ideal displacement model, this sequence reduces interstage liquid remixing and can lower the cycle-average vapor requirement.[1–5]

**Gap.** The nominal operating state is a repeatable VFP–LFP trajectory, not a stationary composition profile. Vapor requirement characterizes separation performance, but it does not show whether this periodic orbit attracts disturbances or how fast the column returns to it.

**Aim.** We formulate one complete cycle as a Poincaré map. Its Floquet multipliers classify local orbital stability, and its dominant eigenvector and decay rate identify the spatial structure and time scale of slow recovery.[6,7]

## CASE 1 | PERIODIC OPERATION

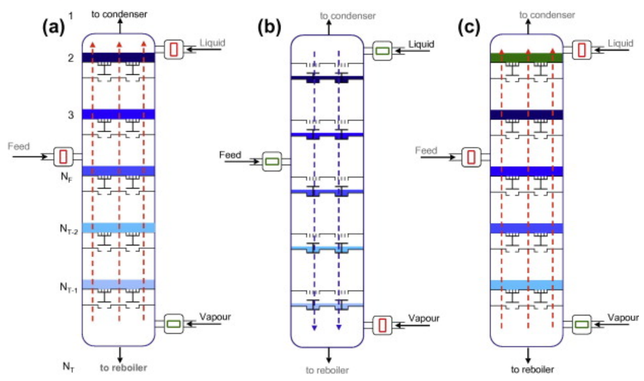


**Two-period sequence.** Vapor contacts the retained liquid during the VFP; the LFP then displaces liquid downward and withdraws products. **Benchmark:** $N = 9$, $n_f = 5$, $\alpha = 3.5$, $t_V/t_L = 12/3$ s. At equal average vapor input, cyclic operation gives $(x_D, x_B) = (0.9962, 0.0047)$ versus $(0.9616, 0.0384)$ continuously.

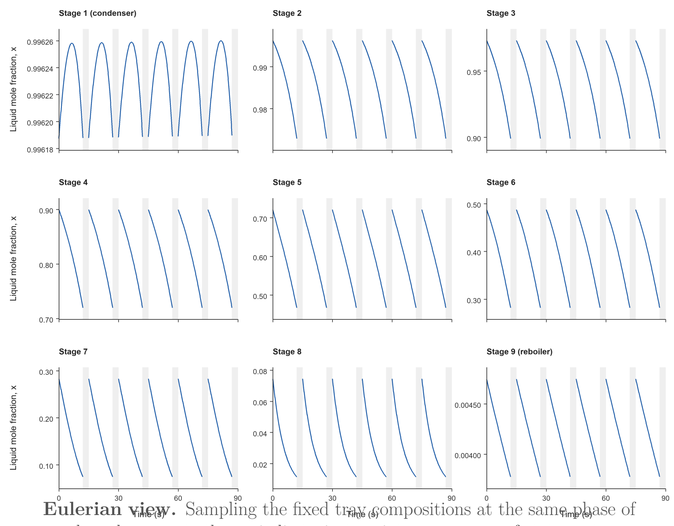


**Eulerian view.** Sampling the fixed tray compositions at the same phase of each cycle converts the periodic trajectory into a sequence of state vectors.

## CASE 2 | RELATIVE VOLATILITY

This case asks whether the lower vapor requirement of cyclic operation persists as the separation difficulty changes. The feed is fixed at $\bar{F} = 0.0250$ kmol/s with $x_F = 0.5$, and both columns must meet the same targets, $x_D = 0.995$ and $x_B = 0.005$. Only the relative volatility is scanned.

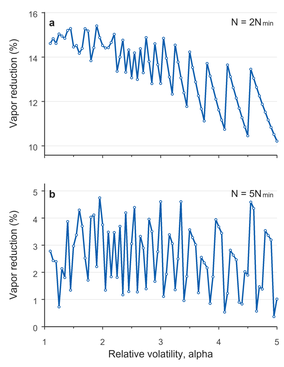


$\alpha = 1.10$–$5.00$

79 points per scan

$N = \lceil 2N_{\min} \rceil$:
**10.20–15.40%**

$N = \lceil 5N_{\min} \rceil$:
**0.37–4.74%**

Base case:
**14.23% reduction**

At fixed $\alpha = 3.5$ and $n_f = 10$, increasing $N = 15 \rightarrow 19$ reduces the advantage from **27.64% to 9.65%**.

$\eta_V = 100(1 - \bar{V}_{\mathrm{cyc}}/V_{\mathrm{conv}})$ is the relative reduction in calculated cycle-average molar vapor requirement, not a thermodynamic efficiency.

## CASE 3 | VFP/LFP DURATION

This case isolates cycle timing from the volatility and stage-selection effects in Case 2. The base separation is fixed at $\alpha = 3.5$, $N = 17$, $n_f = 10$, $\bar{F} = 0.0250$ kmol/s, $x_F = 0.5$, $x_D = 0.995$, and $x_B = 0.005$. Because the ideal LFP is an algebraic displacement event, $t_L = 3$ s is fixed while $t_V$ is varied.

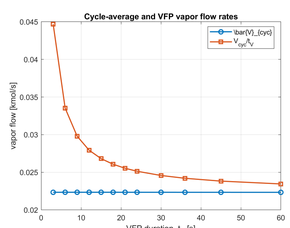


$t_V = 3$–$60$ s

$\bar{V}_{\mathrm{cyc}} \approx$ **0.02235** kmol/s and changes by $<$ 0.05%.

Per-cycle vapor amount:
**0.13405** $\rightarrow$ **1.40720** kmol/cycle.

Instantaneous VFP flow:
**0.044682** $\rightarrow$ **0.023453** kmol/s.

Longer VFPs spread the required vapor over more contact time: the average requirement stays almost unchanged while instantaneous loading falls. Actual flooding, entrainment, weeping, and drainage limits require tray geometry and fluid-property data and are not predicted here.

## CASES 2–3 | DESIGN READING

| Decision | Quantitative result | Design meaning |
|---|---|---|
| **Stage count** | $N = \lceil 2N_{\min} \rceil$: **10.20–15.40%** reduction. $N = \lceil 5N_{\min} \rceil$: **0.37–4.74%**. | The finite-stage vapor advantage decreases as the cyclic column approaches its high-stage limit. |
| **Cycle timing** | $t_V = 3$–$60$ s changes $\bar{V}_{\mathrm{cyc}}$ by $<$ 0.05%, but lowers instantaneous VFP flow from **0.04468** to **0.02345** kmol/s. | Cycle duration redistributes vapor within the imposed sequence rather than changing its average requirement. |
| **Design and reporting** | Optimize $N$ and $n_f$ for vapor screening; select $t_V$ against allowable instantaneous loading. Report $\eta_V$, $\bar{V}_{\mathrm{cyc}}$, stage-count basis, and VFP/LFP timing. | Stage count sets the vapor advantage; timing sets how vapor is delivered. The result is not a heat-duty or thermodynamic-efficiency prediction. |
| **Model boundary** | Ideal binary VLE, constant relative volatility, CMO, and prescribed liquid displacement. | Hydraulic feasibility still requires tray geometry, fluid properties, flooding, weeping, entrainment, and drainage data. |

## POINCARÉ MAP & BASE CASE

**Objective.** Determine whether the optimized periodic orbit attracts composition perturbations, how rapidly it recovers, and where its slowest spatial mode is concentrated.

Sample the fixed-stage composition vector at the start of each VFP. One complete VFP–LFP sequence defines the return map

$$\boldsymbol{x}^{k+1} = \mathcal{P}(\boldsymbol{x}^k), \qquad \boldsymbol{x}^\star = \mathcal{P}(\boldsymbol{x}^\star).$$

The variational VFP and differentiated LFP reset give

$$\boldsymbol{J}_x = \boldsymbol{H}_z \boldsymbol{R}_z \boldsymbol{S}_V(t_V) \boldsymbol{Z}_x, \qquad \rho = \max_j |\lambda_j(\boldsymbol{J}_x)|.$$

Local orbital stability requires $\rho < 1$; $N_{1\%} = \ln(0.01)/\ln \rho$.[6,7]

## CASE 4 | BASE-CASE LOCAL STABILITY

### A FLOQUET MULTIPLIERS

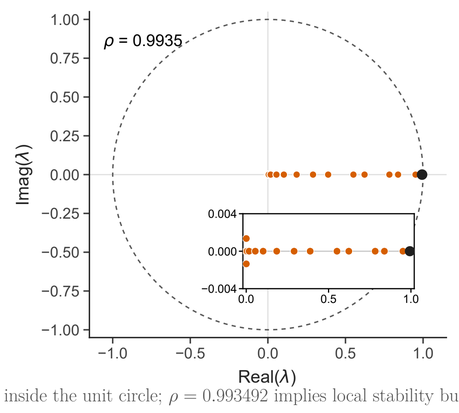


All multipliers lie inside the unit circle; $\rho = 0.993492$ implies local stability but weak attraction.

### B DOMINANT SPATIAL MODE

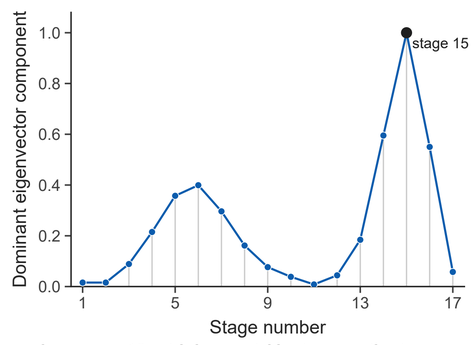


The slow mode peaks at stage 15, with large neighboring contributions at stages 14 and 16.

$\rho = 0.993492$ | $N_{1\%} = 705.32$ **cycles** | $t_{1\%} = 2.94$ **h**

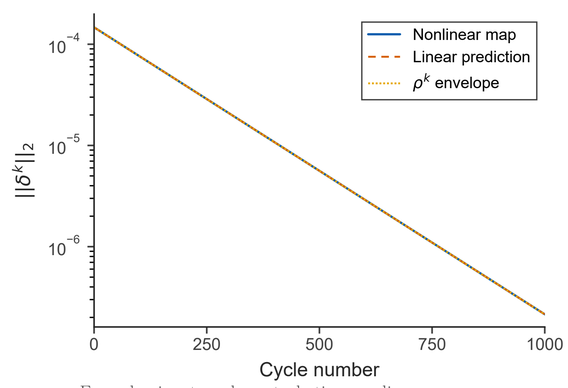


For a dominant-mode perturbation, nonlinear recovery, the linear map, and the $\rho^k$ reference decay nearly coincide.

## CASE 5 | RELATIVE VOLATILITY AND STABILITY

Using the optimized stage number and feed location from Case 2, this case asks how separation difficulty changes the local attraction of the periodic orbit. The product specifications and cycle time remain fixed; the Poincaré map is recomputed for each $\alpha$.

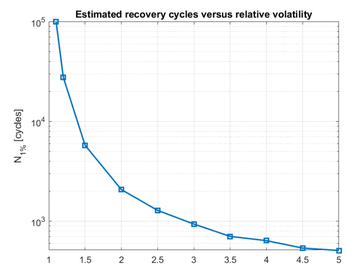


**Close-boiling:** $\alpha = 1.1$
$N = 223$, $n_f = 113$
$\rho = 0.999954$
$N_{1\%} = 100{,}683.69$ cycles
$t_{1\%} =$ **419.52** h

**Wide-boiling:** $\alpha = 5.0$
$N = 14$, $n_f = 8$
$\rho = 0.991001$
$t_{1\%} =$ **2.12** h

### TEN OPTIMIZED PERIODIC STATES

| $\alpha$ | $N$ | $n_f$ | $\rho$ | $N_{1\%}$ [cycles] | $t_{1\%}$ [h] |
|---|---|---|---|---|---|
| 1.1 | 223 | 113 | 0.999954 | 100,683.69 | 419.52 |
| 1.2 | 117 | 60 | 0.999834 | 27,719.42 | 115.50 |
| 1.5 | 53 | 28 | 0.999204 | 5,781.94 | 24.09 |
| 2.0 | 31 | 17 | 0.997789 | 2,080.32 | 8.67 |
| 2.5 | 24 | 13 | 0.996425 | 1,286.03 | 5.36 |
| 3.0 | 20 | 11 | 0.995102 | 937.92 | 3.91 |
| **3.5** | **17** | **10** | **0.993492** | **705.33** | **2.94** |
| 4.0 | 16 | 9 | 0.992828 | 639.82 | 2.67 |
| 4.5 | 15 | 9 | 0.991493 | 539.03 | 2.25 |
| 5.0 | 14 | 8 | 0.991001 | 509.46 | 2.12 |

All ten states satisfy $\rho < 1$. The dominant multiplier is real and positive, so the slowest return is monotonic; however, the recovery time increases by more than two orders of magnitude as $\alpha$ approaches unity.

**Local stability does not guarantee operationally fast recovery.**

## PURITY, DISTURBANCES & DESIGN

### CASE 6 | PRODUCT PURITY

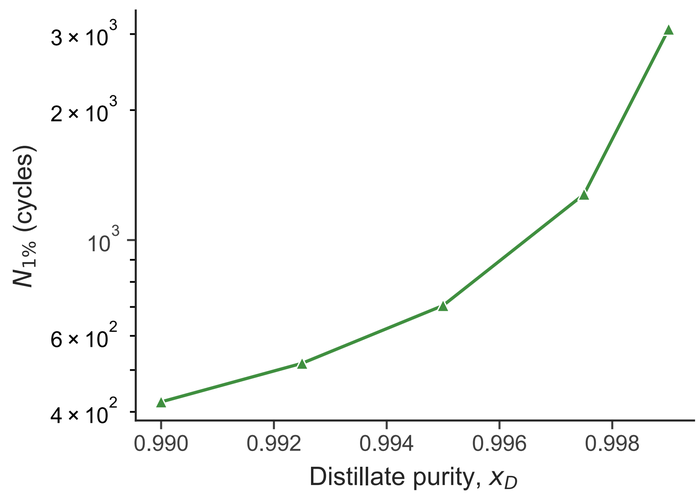


Tightening $(x_D, x_B)$ from $(0.990, 0.010)$ to $(0.999, 0.001)$ changes

$$\rho : 0.98914 \rightarrow 0.99851, \qquad t_{1\%} : 1.76 \rightarrow 12.83 \text{ h}.$$

The cycle-average vapor rate increases only from 0.02208 to 0.02279 kmol/s. High purity therefore carries a much larger recovery penalty than vapor penalty. The slow mode also spreads from the lower stripping section toward the rectifying section and column boundaries.

### FIVE PURITY SPECIFICATIONS

| $x_D$ | **.9900** | **.9925** | **.9950** | **.9975** | **.9990** |
|---|---|---|---|---|---|
| $\bar{V}_{\mathrm{cyc}}$ | .02208 | .02221 | .02235 | .02253 | .02279 |
| $t_{1\%}$ [h] | 1.76 | 2.16 | 2.94 | 5.32 | 12.83 |

### CASE 7 | NONLINEAR DISTURBANCE RECOVERY

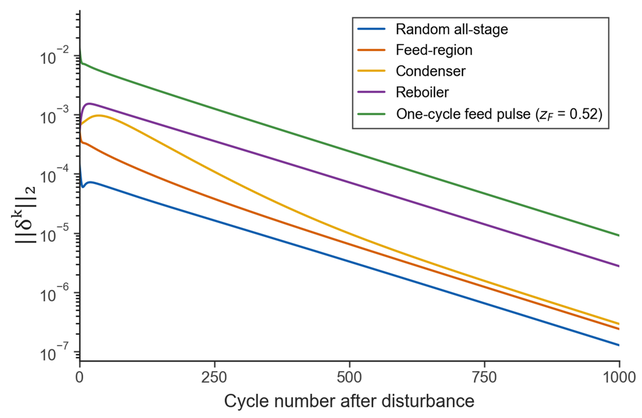


Five tests were applied: normalized random all-stage, feed-region, condenser, reboiler, and a one-cycle feed pulse $x_F : 0.50 \rightarrow 0.52$. All return to the same periodic orbit. Condenser and reboiler perturbations show short-time amplification before asymptotic decay.

The maximum nonlinear–linear relative norm error is $<$ 1%; the largest is **0.82%** for the feed pulse. This validates the local map for the tested finite disturbances, not global stability.

### FIVE DISTURBANCE TESTS

| Test | Imposed magnitude | $\|\delta^{1000}\|_2$ | Max. error |
|---|---|---|---|
| Random all-stage | $10^{-4}$ (max stage) | $1.29\times10^{-7}$ | 0.16% |
| Feed-region | $5\times10^{-4}$ | $2.41\times10^{-7}$ | 0.097% |
| Condenser | $-5\times10^{-4}$ | $2.94\times10^{-7}$ | 0.28% |
| Reboiler | $5\times10^{-4}$ | $2.77\times10^{-6}$ | 0.42% |
| Feed pulse | $\Delta x_F = 0.02$ | $9.12\times10^{-6}$ | 0.82% |

## DESIGN IMPLICATIONS

**1.** Report cycle-average vapor requirement and recovery together.

**2.** Use $\rho$ for local classification, but use $N_{1\%}$ or $t_{1\%}$ to communicate operational recovery.

**3.** The dominant eigenvector identifies the tray region supporting the slow mode; it does not by itself complete sensor or controller design.

**4.** Compare $t_{1\%}$ with the allowable off-spec interval; if recovery is too slow, change the operating policy or develop closed-loop control.

**Closed-loop extension.** The local return map gives the state dynamics needed for a future feedback formulation:
$\delta x^{k+1} = (J_x + B_u K)\, \delta x^k$.

The present study supplies $J_x$; controller synthesis additionally needs $B_u$, measurement timing, estimation, constraints, and actuator dynamics.

**Transient growth.** The $\rho^k$ curve is an asymptotic reference, not a strict norm bound. Here $\kappa(V) \approx 2.7 \times 10^8$ and $\|J_x\|_2 \approx 1.35 > 1$ although $\rho = 0.99349 < 1$; non-normality explains the short-time amplification.

## CONCLUSIONS

**1.** The finite-stage vapor-requirement reduction is **10.20–15.40%** at $N = \lceil 2N_{\min} \rceil$, but only **0.37–4.74%** at $N = \lceil 5N_{\min} \rceil$; changing $t_V$ redistributes instantaneous vapor while changing $\bar{V}_{\mathrm{cyc}}$ by $<$ 0.05%.

**2.** All optimized periodic states examined are locally stable: every Floquet multiplier lies inside the unit circle.

**3.** The base case is stable but weakly attracting: $\rho = 0.993492$, $N_{1\%} = 705.32$ cycles, and $t_{1\%} =$ 2.94 h; the slow mode is concentrated near stage 15.

**4.** Separation difficulty controls recovery: $\alpha = 1.1$ requires 419.52 h, while $(x_D, x_B) = (0.999, 0.001)$ requires 12.83 h. Vapor reduction and recovery speed must therefore be reported together.

**5.** The local map predicts all five tested nonlinear recoveries with $<$ 1% relative norm error. Feedback-control design remains future work.

## REFERENCES

**[1]** Cătălin Pătruţ, Costin Sorin Bîldea, Ionela Liţă, Anton A. Kiss, "Cyclic distillation – Design, control and applications," *Separation and Purification Technology* **125** (2014) 326–336. DOI: 10.1016/j.seppur.2014.02.006.

**[2]** Costin S. Bîldea, Cătălin Pătruţ, Sten Bay Jørgensen, Jens Abildskov, Anton A. Kiss, "Cyclic distillation technology – a mini-review," *Journal of Chemical Technology & Biotechnology* **91**(5) (2016) 1215–1223. DOI: 10.1002/jctb.4887.

**[3]** Vladimir N. Maleta, Anton A. Kiss, V. M. Taran, Bogdan V. Maleta, "Understanding process intensification in cyclic distillation systems," *Chemical Engineering and Processing – Process Intensification* **50**(7) (2011) 655–664. DOI: 10.1016/j.cep.2011.04.002.

**[4]** Bogdan V. Maleta, Alexander Shevchenko, Olesja Bedryk, Anton A. Kiss, "Pilot-scale studies of process intensification by cyclic distillation," *AIChE Journal* **61**(8) (2015) 2581–2591. DOI: 10.1002/aic.14827.

**[5]** Rasmus Fjordbak Nielsen, Jakob Kjøbsted Huusom, Jens Abildskov, "Driving Force Based Design of Cyclic Distillation," *Industrial & Engineering Chemistry Research* **56**(38) (2017) 10833–10844. DOI: 10.1021/acs.iecr.7b01116.

**[6]** John Guckenheimer, Philip Holmes, *Nonlinear Oscillations, Dynamical Systems, and Bifurcations of Vector Fields*, Springer, New York, 1983.

**[7]** Giorgos Kolios, Dan Luss, Rahul Garg, Gautham A. Viswanathan, "Efficient computation of periodic state of cyclic fixed-bed processes," *Chemical Engineering Science* **101** (2013) 90–98. DOI: 10.1016/j.ces.2013.06.029.

**[8]** Tony Joseph Mathew, Mohit Tawarmalani, Rakesh Agrawal, "Relaxing the constant molar overflow assumption in distillation optimization," *AIChE Journal* **69**(9) (2023) e18125. DOI: 10.1002/aic.18125.

**[9]** Jess Bjørn Rasmussen, Seyed Soheil Mansouri, Xiangping Zhang, Jens Abildskov, Jakob Kjøbsted Huusom, "A mass and energy balance stage model for cyclic distillation," *AIChE Journal* **66**(8) (2020) e16259. DOI: 10.1002/aic.16259.